Undulatory Swimming Performance and Body Stiffness Modulation in a Soft Robotic Fish-Inspired Physical Model

Article · March 2017

DOI: 10.1089/soro.2016.0053.

CITATIONS
5

READS
516

4 authors, including:

Ardian Jusufi
Harvard University
30 PUBLICATIONS **692** CITATIONS

SEE PROFILE

George V. Lauder
Harvard University
378 PUBLICATIONS **23,569** CITATIONS

SEE PROFILE

SOFT ROBOTICS
Volume 00, Number 00, 2017

DOI: 10.1089/soro.2016.0053

SoRo
Soft Robotics

ORIGINAL ARTICLE

Undulatory Swimming Performance and Body Stiffness Modulation in a Soft Robotic Fish-Inspired Physical Model

Ardian Jusufi,[1,2] Daniel M. Vogt,[2] Robert J. Wood,[2] and George V. Lauder[3]

Abstract

Undulatory motion of the body is the dominant mode of locomotion in fishes, and numerous studies of body kinematics and muscle activity patterns have provided insights into the mechanics of swimming. However, it has not been possible to investigate how key parameters such as the extent of bilateral muscle activation affect propulsive performance due to the inability to manipulate muscle activation in live, freely swimming fishes. In this article we extend previous work on passive flexible mechanical models of undulatory propulsion by using actively controlled pneumatic actuators attached to a flexible foil to gain insight into undulatory locomotion and mechanisms for body stiffness control. Two soft actuators were attached on each side of a flexible panel with stiffness comparable to that of a fish body. To study how bilateral contraction can be used to modify axial body stiffness during swimming, we ran a parameter sweep of actuator contraction phasing and frequency. Thrust production by the soft pneumatic actuators was tested at cyclic undulation frequencies ranging from 0.3 to 1.2 Hz in a recirculating flow tank at flow speeds up to 28 cm/s. Overall, this system generated more thrust at higher tail beat frequencies, with a plateau in thrust above 0.8 Hz. Self-propelled speed was found to be 0.8 foil lengths per second or $\sim$13 cm/s when actuated at 0.55 Hz. This active pneumatic model is capable of producing substantial trailing edge amplitudes with a maximum excursion equivalent to 1.4 foil lengths, and of generating considerable thrust. Altering the extent of bilateral co-contraction in a range from −22% to 17% of the cycle period showed that thrust was maximized with some amount of simultaneous left-right actuation of $\sim$3% to 6% of the cycle period. When the system is exposed to water flow, thrust was substantially reduced for conditions of greatest antagonistic overlap in left-right actuation, and also for the largest latencies introduced. This experimental platform provides a soft robotic testbed for studying aquatic propulsion with active control of undulatory kinematics.

Keywords: soft, undulation, swimming, fish, co-contraction, stiffness, pneumatic, robot

Introduction

STUDIES OF AQUATIC PROPULSION in fishes have focused for many years on quantifying patterns of body bending, and understanding how the segmented body musculature (myotomes) generates the variety of kinematic patterns observed during locomotion.[1–3] Analyses of fish kinematics and motor patterns have considered diverse fish species, including forms as disparate as eels, largemouth bass, trout, and sharks and rays,[4–7] and compared kinematic and muscle activity patterns among species. These studies have provided a wealth of information on how electrical activity is propagated down the body, the phase relationship between body bending and muscle activation during swimming, analyses of correlated fin and body motion, and how differently shaped fishes diverge (or not) in swimming kinematics.

Due in part to limitations on the kinds of behaviors that fishes can be voluntarily induced to perform in the laboratory

[1]Centre for Autonomous Systems, Faculty of Engineering and Information Technology, University of Technology, Sydney.
[2]Wyss Institute for Biologically Inspired Engineering, School of Engineering and Applied Sciences, Harvard University, Cambridge, Massachusetts.
[3]Department of Organismic and Evolutionary Biology, Harvard University, Cambridge, Massachusetts.

and constraints on experimental measurements that can be done on freely swimming animals, researchers have turned in recent years to physical models of swimming systems to better understand the mechanisms of aquatic propulsion. Altering body stiffness, for example, in a fish that is freely swimming, is not a practical experimental approach to understanding how stiffness affects propulsive performance. Many recent studies have focused on the analysis of simple passively flexible models (e.g., Refs.[8–12]). These flexible panel or foil studies have the advantage of using a simple model system where the foil is actuated by motors that drive the leading edge in pitch (rotation), heave (side to side motion), or both. Panels are typically held in place by the leading edge shaft, and analysis of forces and torques generated during swimming has provided a wealth of information about locomotor dynamics. For example, Shelton and Lauder[12] analyzed the effect of changing the stiffness of a flexible fish-sized rectangular foil on propulsive efficiency, and Lucas et al.[13] considered the effect of nonuniform stiffness distributions on propulsion. Witt *et al.*[14] used passively flexible plastic panels to model the rapid escape response of fishes.

These swimming panel systems are simple to construct, and avoid most of the challenges involved in constructing a more biomimetic fish-like design. However, while simple foil systems allow focus on some of the key parameters that may influence swimming performance such as body stiffness, the kinematic patterns generated during locomotion are the result of interaction between water and the passively bending foil, not from active bending along the body as occurs in swimming fishes. At the other end of the complexity spectrum are freely swimming robotic fish-like designs (see reviews of fish robotic systems in Ref.[15]), including tendon-driven robots (e.g., Ref.[16]) and soft hydraulic platforms,[17] which represent a more intricate system involving considerable manufacturing challenges. Autonomous robotic fish provide a more biomimetic platform for examining three-dimensional (3D) maneuverability and the evaluation of swimming performance based on a fully realized fish-like body shape, but conducting detailed performance tests and quantifying locomotor forces on freely swimming bodies is also challenging. And iterating such complex designs to evaluate alternative structures or actuation strategies is much more time consuming than with simpler systems.

In this article, our overall aim is to introduce the design and testing of an experimental platform that possesses some of the advantages of previous passive foil systems, and yet incorporates an active segmented fish muscle-like actuation system to provide for controlled bending and propulsion. Forces generated by this experimental platform are due to active bending of the foil propulsor, and they are not provided by external heave and pitch motors. This abstracted fish-like test system is considerably simpler than fully autonomous fish-like robotic platforms, while simultaneously reducing manufacturing complexity, iteration time, and simplifying force and kinematic measurement.

Our specific goals here are, first, to present the development of a soft-robotic fish-like experimental platform that extends previous work on passive flexible foils by using an active pneumatically controlled and segmented bending actuator on both sides of a simple flexible ''backbone.'' Second, we evaluate the thrust-generating capabilities of this system to determine whether these pneumatic actuators are able to generate sufficient thrust to provide self-propulsion at slow to moderate fish-like swimming speeds. Our pneumatic model represents an abstraction of a generalized perciform fish-like body (such as a largemouth bass, *Micropterus salmoides*, and sunfish, *Lepomis macrochirus*) swimming in a body-caudal fin undulatory mode (see Ref.[18] for a review and discussion of fish swimming modes). Third, we evaluate the effects of changing co-activation of the left and right sides of our swimming model to determine how the extent of right-left co-activation and hence body stiffening affects thrust generation, as has been hypothesized previously for models of fish locomotion.

We anticipate that experimental tests with this type of physical model could be useful for testing the effect of changing control patterns in body-caudal fin fish propulsion, and that future extensions of this platform will allow modular addition and control of additional segmental elements. This would enable a diversity of fish locomotor modes ranging from anguilliform to sub-carangiform to thunniform locomotion to be studied. This type of model can also be useful to study fish propulsion over a range of body sizes, made feasible by progressive miniaturization of soft pneumatic actuators that are presently under development for surgical procedures.

Materials and Methods

Development of the physical model

Soft actuators consisted of a cured silicone-based elastomer. We manufactured the soft actuators with uncured elastomers and molds utilizing the techniques described by Mosadegh *et al.*[19] These authors have also described the characteristics of such soft actuators, including their dynamic speeds and limitations. The manufacturing process we selected is illustrated as follows. Before pouring an elastomeric material in the 3D-printed (Objet Geometries, Billerica, MA) mold (Fig. 1A) we apply release spray onto the interior walls of each chamber. Once poured, we place the silicone elastomer in an oven and cure it at a temperature of 60°C for a duration of 20 min. After having removed the part from the mold we pour a fresh, thin layer of elastomeric material on the base mold (Fig. 1B). Next, we lay the previously molded part on the uncured elastomer and let it cure at room temperature for at least 4 h (Fig. 1C). We then removed the actuator from the mold. To provide an air inlet for the plumbing we punch a hole on the anterior chamber and test the actuator by pressurizing. Last, we glue two soft pneumatic actuators bilaterally onto the foil with a silicone epoxy (Silpoxy®; Smooth-On, Inc., Easton, PA). The actuators were 10 cm long and 2 cm in height.

This design produced a segmented, chambered soft actuator that allowed smooth bending patterns to be generated along a relatively stiff but flexible central ''backbone'' panel. Two such pneumatic soft actuators were attached bilaterally on each side of a flexible foil with stiffness comparable to a fish body, and they were used to generate undulatory motions of this central panel (Fig. 1E). The flexible foil or panel material used was the 0.52 mm thick shim stock (Artus, Inc.) that has been used as a physical model of passive propulsion in several previous studies and has a measured Young's modulus of 1240 MPa.[12] These authors also reported a flexural stiffness of $9.9 \times 10{-}4$ N m^2 for this material of similar

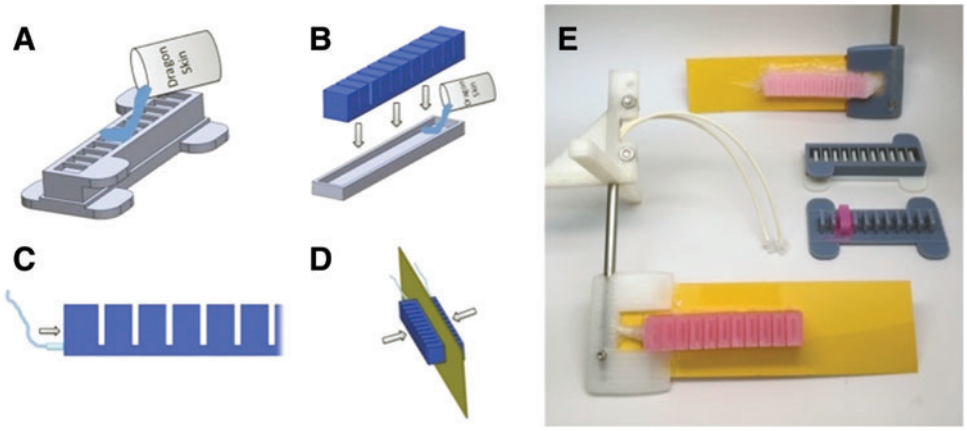

FIG. 1. Manufacturing technique for soft pneumatic actuators utilized in undulating platform. Elastomeric material is poured into a chambered mold. Material is cured at 60°C for 20 min **(A)**. Upper chambered part is removed from the mold. Fresh elastomeric material Dragon Skin is poured onto the base mold. The previously molded part is placed on the uncured elastomer and it is subsequently cured at room temperature for a minimum of 4 h **(B)**. The actuator is extracted from the mold. To pressurize the actuator a hole is punched for the air inlet and plumbing **(C)**. The actuator is glued onto the foil with a silicone epoxy **(D)**. All the components used in the manufacturing process **(A–D)** are depicted in the photograph along with the final soft robotic fish-like physical model **(E)**. Color images available online at www.liebertpub.com/soro

dimension to that used here: the backbone panel had dimensions of 17 cm in length, and 5.94 cm in height. The silicon elastomer that we used to make the soft actuators has a tensile strength of 550 psi (3.792×10^6 Pa), and 310 kPa for 100% modulus (Smooth-On, Inc.).

Device control and operation was designed such that the microcontroller circuit board (Arduino, Nano, SmartProjects, Italy), pressure sensor (BSP B010-EV002-A00A0B-S4; Balluff, Inc., Florence, KY), pressure regulator, and solenoid valves (Parker V2 Miniature Pneumatic Solenoid Valve) were placed off-board. Pulse-width modulation control was used to control the phasing of actuator pressurization to generate the desired undulatory motion patterns. The system was pressurized using compressed air ranging from 40 to 150 kPa (0.4 to 1.5 bar, respectively).

Data acquisition and analysis

Kinematic data were acquired through high-speed videography (Fig. 2) utilizing a Photron PCI-1024 system (one megapixel resolution) at a frame rate of 250 frames per second. Swimming motion was filmed from below simultaneously with recordings of thrust forces generated as the pneumatic actuator system swam in a recirculating flow tank.

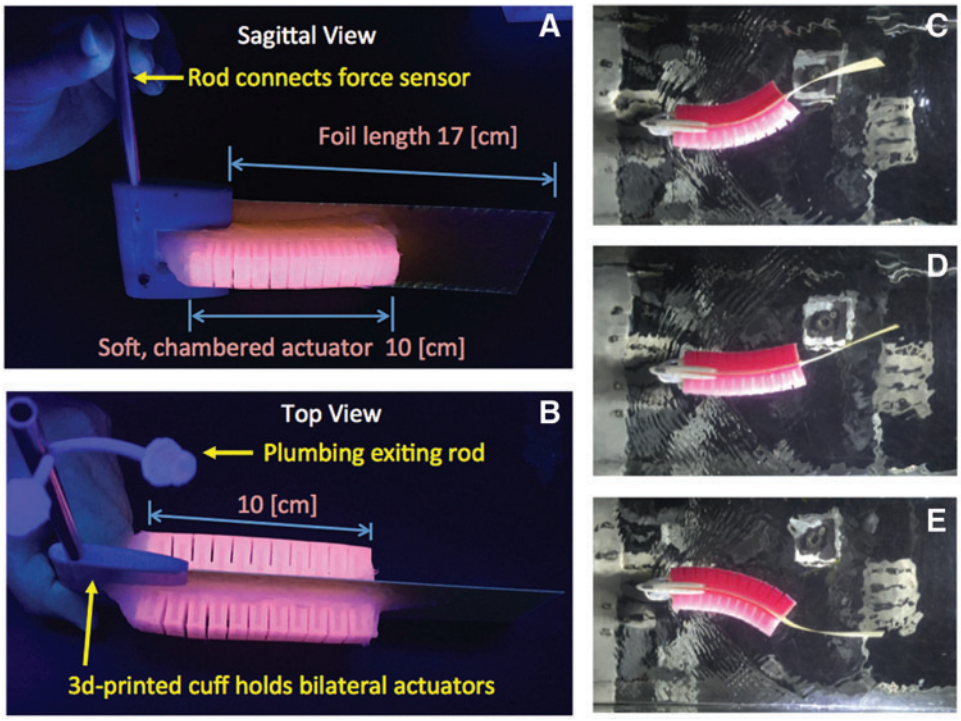

FIG. 2. Undulating soft robotic fish-like model of axial musculature with two soft pneumatic actuators connected to a rod via a three-dimensional (3D)-printed cuff. Displayed in **(A)** sagittal view and **(B)** *top* view under ultraviolet light to emphasize the segmented pneumatic actuators. *Side* view of 3D-printed cuff holding the foil and actuator. **(C–E)** Motion sequence showing *left-right* bending of the bilateral actuators and central foil ''backbone'' to the *left* and *right*. See Supplementary Movie S1 for undulatory motion pattern. Color images available online at www.liebertpub.com/soro

This flow tank, with working section dimensions of 26 cm by 26 cm by 80 cm, was the same one used previously for studies of passively swimming physical models, and for analyses of fish swimming kinematics and muscle activity (e.g.,[6,11,12,20–23]). Flow speed was altered between 0 and 20 cm/s, which represents slow to moderate relative swimming speeds for bodies of our actuator length, and these speeds represent typical routine fish undulatory swimming speeds in nature. Flow speed was altered in different trials to determine the relationship between thrust forces generated and flow speed as described below. Backbone undulation generated by the pneumatic actuators was studied at frequencies ranging from 0.3 to 1.2 Hz. These frequencies also correspond to slow to moderate fish swimming frequencies, although at higher speeds and during unsteady behaviors such as escape responses fish movements are of much higher frequency.

For swimming forces to be transferred effectively from the soft pneumatic actuators to the central backbone and supporting rod to generate undulatory kinematics, a stiff cuff holder was required (Figs. 1E and 2A, B). A low profile 3D-printed cuff-like structure was attached to the anterior portion of the foil and a supporting rod attached this cuff to a force transducer above. The soft robotic model with components as illustrated in Figure 1 was mounted in the recirculating flow tank with the force transducer and pneumatic controller located above the water (Fig. 2A, B).

Device development involved generating multiple versions of the undulating fish-like model and exploration of different ways to generate actuation without incurring large drag forces. To reduce drag, the two soft pneumatic actuators were connected to a rod containing the required pneumatic plumbing internally. The supporting rod was attached to a force transducer located above the water level, and this transducer was in turn attached to a rigid aluminum support above the flow tank. To measure thrust during swimming, the supporting rod was attached to a Nano 17 six-axis force/torque sensor (ATI Industrial Automation, Apex, NC). We emphasize that these force measurements were conducted with the ATI transducer fixed in position while actuation occurs on the foil surface that is driven locally: thrust is thus generated actively by the foil itself, and *not* by external motors. These experiments thus contrast with our previous work on passive foil propulsion where an imposed heave and pitch motion drives the passively flexible foil, and the ATI transducer and supporting rod move as oscillatory motion is driven by external heave and pitch motors.

Force measurements were carried out at a sampling rate of 250 Hz. Data analysis and statistics were carried out using Matlab R2015b (The Mathworks). Data acquisition during undulation experiments occurred over the duration of 120 s for each condition investigated. Analysis of force measurements involved taking the mean of five trials, representing thrust measurements collected at a sampling frequency of 250 Hz for a duration of 24 s for each one of the five trials. Error bars in the figures represent standard deviations for each of the mean values.

Thrust force measurements made over a range of flow speeds allow determination of the self-propelled swimming speed for the entire cuff, actuator, and panel complex. Self-propulsion occurs when the mean thrust force over a single undulatory cycle is zero.[10,23] Recording negative thrust values during swimming indicates that the drag of the foil complex at the tested speed exceeds the thrust being generated; net positive thrust reflects a condition where the foil would accelerate were it not attached to a supporting rod that is fixed externally (see Supplementary Movie S1 for undulatory motion pattern powered by soft actuators; Supplementary Data are available online at www.liebertpub.com/soro). Identifying the self-propelled speed and quantifying swimming dynamics at this speed is important because it reveals the threshold at which the thrust generated by the system exceeds the drag incurred at a certain flow speed. Experiments performed in a recirculating flow tank at a range of flow speeds permit characterization of changes in foil kinematics and wake structure that occur in flexible propulsors at nonself-propelled conditions.[10] In addition, it is important to determine whether these pneumatic actuators, when incorporated into our system design, are capable of powering a swimming system at self-propelled speeds.

To measure the effect of co-contracting actuators on the body stiffness the following experiment was performed. The physical model's anterior cuff was fixed with a clamp. While both actuators were pressurized symmetrically a material tester (Instron 5544A; Instron, Norwood, MA) was used to apply a deflection of a known distance to the system while measuring the resistive blocking force as shown in Figure 7A. The experiment was repeated for several pressures up to 40 kPa and data are measured with a sampling frequency of 100 Hz. The force measured for several pressures is shown on Figure 7B. For each curve, the data have been smoothed (moving average with 50 samples) and the slope of each graph (representing the stiffness) was calculated by doing a linear regression. The stiffness values measured at the different pressures (Fig. 7C) can then be compared.

Results

To characterize swimming performance, we investigated the kinematics of the system and measured propulsive forces (see Supplementary Movie S1 for undulatory motion pattern). To test how swimming performance is affected by bilateral contraction under body stiffness modulation, we ran a parameter sweep of actuator contraction phasing and frequency.

When water flow speed was set to zero in the recirculating flow tank, effectively leaving the tail fin in still water, the maximum amplitude of the trailing edge was 1.4 tail lengths (23.73 cm) at the lowest frequency of 0.3 Hz. The amplitude of excursion dropped to 0.96 tail lengths (16.25 cm) at 0.55 Hz and 0.39 tail lengths (6.6 cm) at the highest frequency of 1.2 Hz tested (Fig. 3). Although the control electronics and the valves are capable of operating at higher frequencies, the pneumatic actuator would struggle to follow up with faster switching and it would result in a qualitative decline of the trailing edge amplitude (Fig. 3G). This decline is mostly due to the slow dynamics of the soft flapper when submerged in water and therefore we limited our upper frequency to 1.2 Hz. Additionally, since this series of experiments is not closed loop controlled, the water flow speed can also influence the observed trailing edge kinematics of the tail fin (i.e., amplitude) and therefore affect the swimming performance.

We measured thrust at a range of flow speeds (Fig. 4) and found that the cuff/actuator/foil complex is capable of generating positive thrust at lower flow speeds, negative thrust

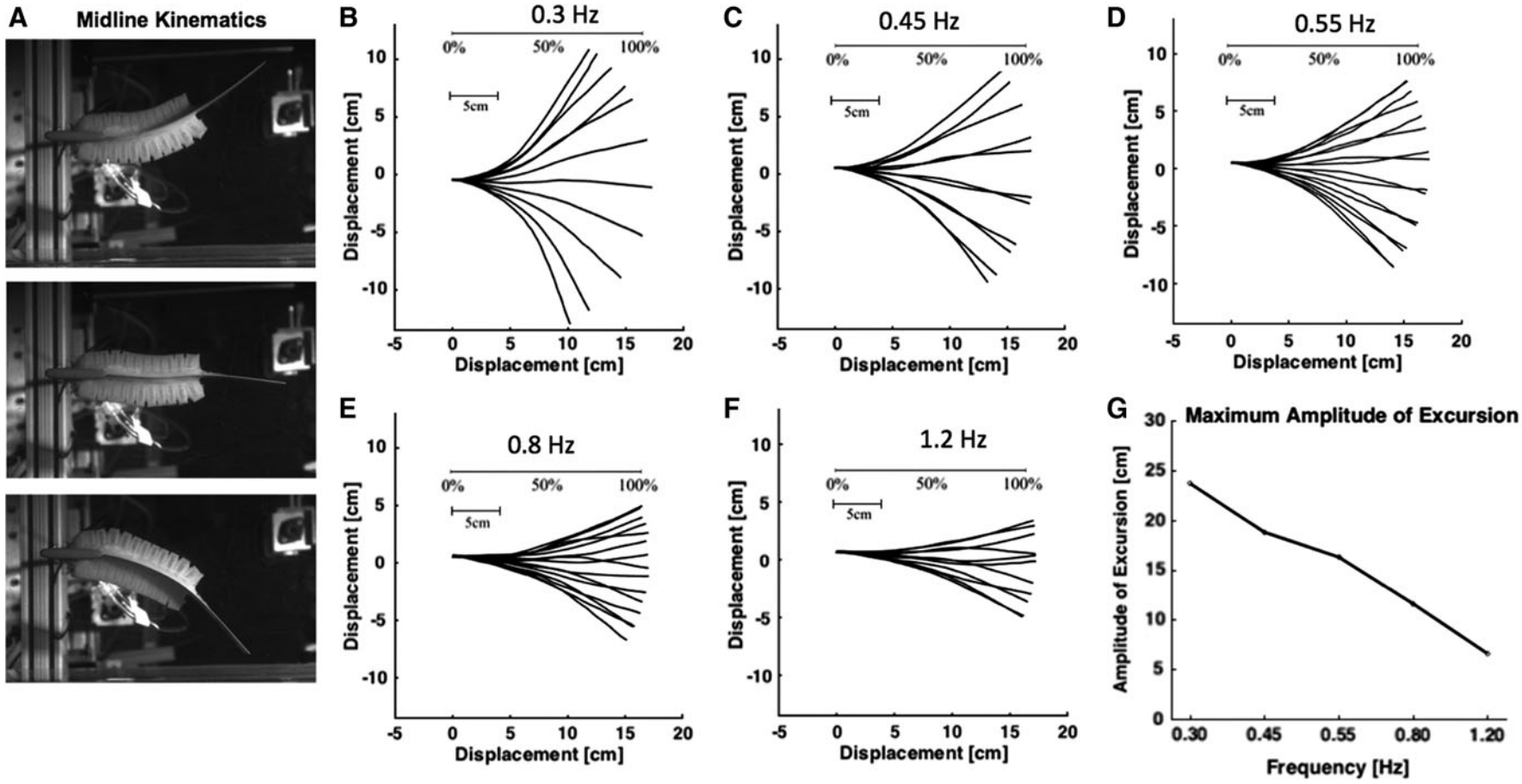

FIG. 3. Midline kinematics at a range of tail-beat frequencies. **(A)** Motion sequence of the soft robotic fish-like physical model with alternating bilateral pressurization of actuators. **(B–F)** Midline motion pattern of foil as imposed by soft actuators where 0% represents the front part of the foil attached to the 3D-printed cuff and rod, and 100% indicates the posterior tip of the plastic foil. Each graph depicts experiments at a different undulation frequency ranging from 0.3 to 1.2 Hz. **(G)** Graph illustrates the maximum total lateral excursion of tail tip relative to foil midline for each undulation frequency tested.

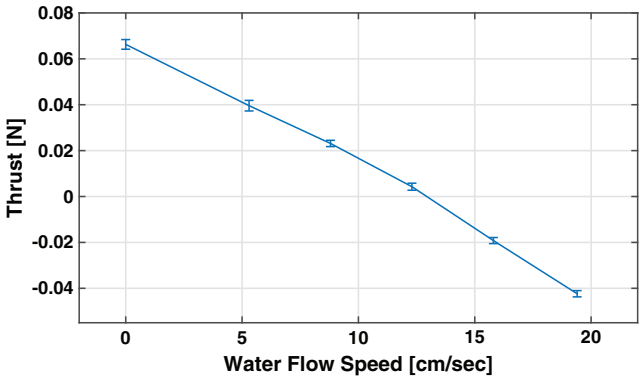

FIG. 4. Thrust measured at a range of flow speeds from 0 to ~20 cm/s in a recirculating flow tank at a foil undulation frequency of 0.55 Hz. The zero-crossing indicates the self-propelled speed of the model, here circa 13 cm/s. Negative thrust values thus indicate that the foil and actuator system was not generating sufficient thrust to overcome drag. Each data point plotted represents the mean value of five trials with force measurements for a duration of 24 s each. Error bars represent the standard deviation for each mean value. Flow speeds corresponded to 5.3, 8.8, 12.3, 15.8, and 19.4 cm/s. Color images available online at www.liebertpub.com/soro

(net drag) at higher flow speeds, with a self-propelled speed equivalent to 0.75 foil lengths per second or ~13 cm/s when the complex is actuated at a frequency of 0.55 Hz.

Moreover, we performed a frequency sweep (Fig. 5) at constant water flow of 5.3 cm/s. Soft pneumatic actuators were tested at cyclic undulation frequencies ranging from 0.3 to 1.2 Hz at pressures from 40 to 150 kPa. Peak thrust reached a plateau at 0.8 Hz above and there was no increase. There was a local maximum at 0.55 Hz, and this could be due to resonance of the actuated complex (Fig. 5). We chose to explore this frequency further with measurements at a range of flow speeds as illustrated in Figure 4.

By introducing a delay or ''dead time'' between pressurizing the left and right side actuators we were able to assess

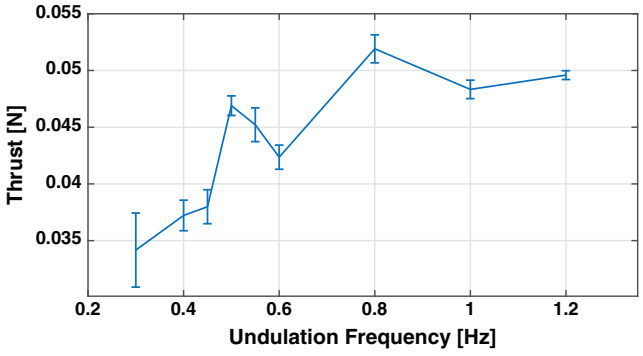

FIG. 5. Thrust measured in a soft robotic fish model undulatory swimming at frequencies ranging from 0.3 to 1.2 Hz at a constant water flow speed of 5.3 cm/s. Each data point plotted represents the mean of five trials with force measurements for a duration of 24 s. Error bars represent the standard deviation of the mean. Color images available online at www.liebertpub.com/soro

the effect of bilateral co-activation on thrust production (Fig. 6). Contraction phasing for left-right side actuation is represented as percent periodic time in Figure 6A to convey the series of experiments with a latency equivalent of 22% cycle period (which corresponds to a ''dead time'' of 400 ms), 16.5% periodic time (300 ms), in addition to 11%, 8.3%, 5.5%, and 2.8% (200, 150, 100, and 50 ms, respectively). Comparing the effects of these ''dead time'' latencies versus simultaneous antagonistic co-contraction illustrated as ''overlap'' (Fig. 6) in terms of how they affect swimming performance, we found the highest thrust at a left-right overlap of 2.8% (50 ms) with thrust decreasing with delays of more than 8.3% of the cycle period (Fig. 6). Thus, altering the extent of bilateral co-contraction from 17% of the cycle period to −22% latency ''dead time'' showed that both for conditions of greatest antagonistic overlap in simultaneous left-right actuation, and the largest latencies induced, thrust was greatly reduced; maximal thrust was produced with a simultaneous left-right co-contraction of 2.8% to 6% of the cycle period.

To determine whether bilateral left-right co-activation has the capability to alter the stiffness of the body, we carried out a set of experiments to measure the stiffness (Fig. 7A). As the soft actuators are co-activated we measured an increase in stiffness that can be observed as a steeper slope when we plot force as a function of extension (Fig. 7A, B). A comparison of the stiffness values illustrated in Figure 7C reveals an

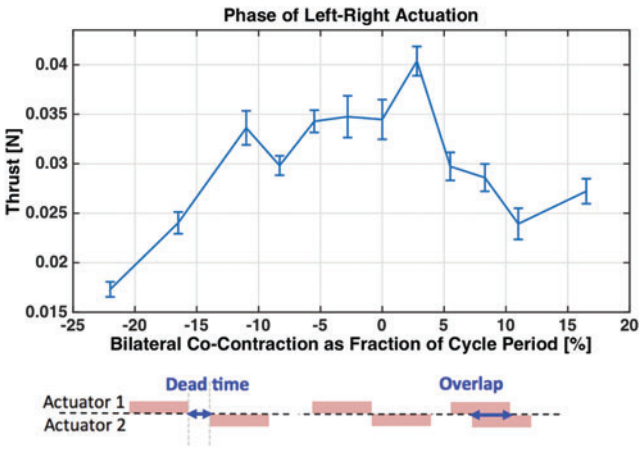

FIG. 6. Measurement of thrust as a function of co-contraction phasing between the *right* and *left* sides in undulatory swimming of a soft robotic fish-like model at 0.55 Hz while exposed to continuous water flow speeds of 5.3 cm/s. Each thrust data point represents a mean over a trial length of 30,000 samples over a total cumulative duration of 120 s from five trials. **(A)**. Contraction phasing for actuation *left-right* side actuation is represented as percent periodic time for experiments with a latency of −22% cycle period or −400 ms, and −300 ms, −200 ms, −150 ms, −100 ms, −50 ms, respectively, with such delay designated as ''dead time''. Overlapping actuation between the *left* and *right* sides is shown as a positive value up to 17% of cycle period, while the extent of nonoverlapping actuation is presented as a negative latency. **(B)** Schematically the pattern of bilateral actuation corresponding to the respective regions in the graph above. Color images available online at www.liebertpub.com/soro

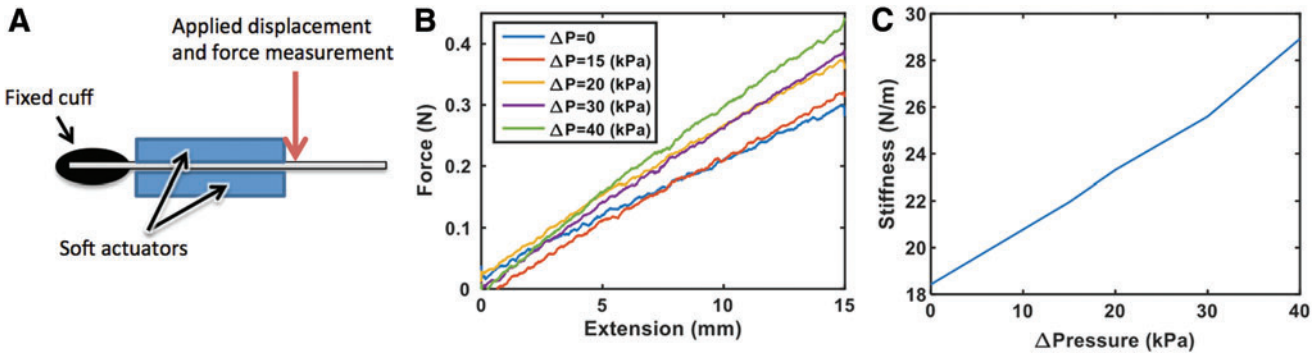

FIG. 7. Experimental setup for measurement of body stiffness under bilateral co-activation with both actuators pressurized symmetrically. **(A)** The soft robotic fish-like model is displaced by a known distance and the resisting force is measured. **(B)** The plot illustrates the block force measured when co-activating the actuators at predetermined pressure values. **(C)** The graph represents the stiffness values of the pneumatic swimmer that are equivalent to the slopes from the force-extension plot. Color images available online at www.liebertpub.com/soro

increase from ~18 to 29 N/m for pressure values of 0, 15, 20, 30, and 40 kPa.

Discussion

In this article we present an experimental platform for investigating several key features of undulatory propulsion in a swimming system that generates locomotor forces using segmented pneumatic actuators attached to a flexible central foil backbone. This test bench offers the unique ability to apply different frequencies and co-contractions in a flexible prototype that can then be compared to fishes. We found that this system is capable of thrust generation and self-propulsion, and evaluated the effects of changing actuation frequency and the amount of antagonistic ''contraction'' between the right and left sides.

Among the most fundamental questions regarding the mechanism of undulatory propulsion is the extent to which active modulation of body stiffness can affect swimming performance,[24–27] and particularly how such modulation affects swimming speed and efficiency. Dynamic tuning of the body stiffness has been hypothesized to substantially reduce the internal resistance to bending considering that matching the body's natural and driving frequencies reduces the force required to cause a given motion independent of the hydrodynamic load.[25] It has also been suggested that speed could be increased by animals as they store and return energy in their body. Specifically, it has been hypothesized that swimming performance could be enhanced with increasing Young's modulus, suggesting that adaptive body stiffness can be used to control swimming speed.[24] For example, a stiffening of body elements could reduce power losses associated with thrust generation at higher frequencies.

Measurements of axial muscle activity along trunk and caudal vertebrae in swimming fish reveal substantial regions of simultaneous activity propagating posteriorly along one side[1,6,28] and this result from live fish is reflected in our actuation of large regions along one side using the segmented pneumatic actuator. Quantitative data on the extent of overlap between left-side and right-side activity are scarce, but some published reports (see Fig. 6 in Ref.[6]) suggest relatively short periods of simultaneous left-right activity at any specific longitudinal location along the body, which corresponds well to our result of maximal thrust when only a short period of co-contraction occurs (Fig. 6A).

External stimulation of muscle was found to increase flexural stiffness in the body, which is hypothesized to be used to match the body resonant frequency with the swimming frequency.[24,25] Theoretical considerations suggest that for an animal to increase swimming speed, it has to either generate more power by increasing frequency or increased stimulation of myotomal musculature, and then transfer this power to thrust production.[24] Moreover, it has been hypothesized that as the bending wave travels passively through the body of a fish, muscle sarcomeres and elastic elements are stretched and when muscle activation occurs during muscle lengthening, stretch activation may enhance power production. It has been established experimentally that eels possess the neuromechanical apparatus for the muscles to be activated as they are lengthened to increase the body stiffness and assist in propagation of the bending wave.[25] Such active lengthening of muscle sarcomeres could decrease the amount of bending thereby inducing stiffening.

Our experimental system generated more thrust at higher tail beat frequencies thus confirming expectations from the literature,[12,24,25] and enabled testing of the effect of changing bilateral overlap (co-contraction) in activation. The pneumatic actuators are capable of generating considerable thrust, particularly when some amount of co-contraction is used in agreement with hypotheses from experiments on swimming fishes.[25–27] Our results point to the importance of co-contraction and the modulation of the body stiffness on swimming performance. Indeed, a small increase of co-contraction can play a significant role in increasing the thrust generated. It is also possible that co-contraction accelerates the transition in the cycle from generating positive thrust to drag at peak amplitude of excursion by reducing the profile exposed to oncoming water flow. The dead time region shown in Figure 6 from −22% to −6% (−400 to −100 ms, respectively) of cycle period exhibited the lowest thrust, indicating that no co-contraction results in worst swimming performance. Large latencies at peak excursion may increase drag, particularly when exposed to flow. A small amount of co-activation on the right and left sides in the region of ~3%

to 6% of periodic time generated the greatest thrust with this simple physical model, but it remains to be seen if this result holds when more complex patterns of actuation are imposed. We made an effort to reduce drag in our experimental system by streamlining the leading cuff that holds the foil and actuators, but we did not attempt to streamline the actuators themselves to reduce their projected area. Despite the increased drag undoubtedly caused by the segments projecting laterally into the flow, considerable thrust was generated and future efforts to streamline the actuators themselves by modifying aspect ratio will certainly increase self-propelled swimming speeds.

The use of segmented pneumatic actuators provided a smooth pattern of bending in the central foil ''backbone'' since these actuators can apply a more even force distribution along the foil's longitudinal axis. Moreover, this strategy holds promise for extension into more complex segmented designs in future iterations of this platform. In particular, we believe that the generation of more complex backbone waveforms by adding additional pneumatic elements lengthwise will provide more eel-like body waveforms (see Refs.[21,29–31]) and will allow us to study the effect of different patterns of actuation and bending propagation on thrust generation.

Beyond generating thrust, soft actuators could also enhance maneuverability by controlling continuous shape changes that are more appropriate for motions such as rapid inversion of body orientation.

In this spirit, we anticipate that soft actuators and sensors will play a role in complementing and building upon important contributions described in the literature (Ref.[31] for a recent example) in deciphering how stiffness affects swimming performance in conjunction with damping and internal dynamics.

Acknowledgments

We are grateful to two anonymous reviewers for their help in improving upon the manuscript. We thank K.N. Lucas for valuable insights. We are grateful for support from the Swiss National Science Foundation for a grant to A.J., the Wyss Institute for Biologically Inspired Engineering at Harvard University, and the Office of Naval Research grant ONR N00014-0910352 to G.V.L.

Author Disclosure Statement

No competing financial interests exist.

References

1. Altringham JD, Ellerby H. Fish swimming: patterns in muscle function. J Exp Biol 1999;202:3397–3403.
2. Lauder GV. Fish locomotion: recent advances and new directions. Ann Rev Mar Sci 2015;7:521–567.
3. Gemballa S, *et al.* Evolution of high-performance swimming in sharks: transformations of the musculotendinous system from subcarangiform to thunniform swimmers. J Morph 2006;267:477–493.
4. Donley JM, Shadwick RE, Sepulveda CA, Konstantinidis P, Gemballa S. Patterns of red muscle strain/activation and body kinematics during steady swimming in a lamnid shark, the shortfin mako (*Isurus oxyrinchus*). J Exp Biol 2005;208:2377–2387.
5. Ellerby DJ, Spierts I, Altringham J. Fast muscle function in the European eel (*Anguilla anguilla L.)* during aquatic and terrestrial locomotion. J Exp Biol 2001;204:2231–2238.
6. Jayne B, Lauder G. Are muscle fibers within fish myotomes activated synchronously? J Exp Biol 1995;198:805–815.
7. Rosenberger LJ. Pectoral fin locomotion in batoid fishes: undulation versus oscillation. J Exp Biol 2001;204:379–394.
8. Dewey PA, Carriou A, Smits AJ. On the relationship between efficiency and wake structure of a batoid-inspired oscillating fin. J Fluid Mech 2012;691:245–266.
9. Dewey PA, Boschitsch BM, Moored KW, Howard AS, Smits AJ. Scaling laws for the thrust production of flexible pitching panels. J Fluid Mech 2013;732:29–46.
10. Lauder GV, Lim J, Shelton R, Witt C, Anderson EJ, Tangorra J. Robotic models for study of undulatory locomotion. Mar Technol Soc J 2011;45:41–55.
11. Quinn DB, Lauder GV, Smits AJ. Maximizing the efficiency of a flexible propulsor using experimental optimization. J Fluid Mech 2015;767:430–448.
12. Shelton RM, Thornycroft PJM, Lauder GV. Undulatory locomotion of flexible foils as biomimetic models for understanding fish propulsion. J Exp Biol 2014;217:2110–2120.
13. Lucas KN, *et al.* Effects of non-uniform stiffness on the swimming performance of a passively-flexing, fish-like foil model. Bioinspir Biomim 2015;10:056019.
14. Witt WC, Wen L, Lauder GV. Hydrodynamics of c-start escape responses of fish as studied with simple physical models. Integr Comp Biol 2015;55:728–739.
15. Du R, Li Z, Youcef-Toumi T, Alvarado PV. Robot Fish: Bio-inspired Fishlike Underwater Robots. Berlin: Springer, 2015.
16. Epps BP, Valdivia y Alvarado P, Youcef-Toumi K, Techet AH. Swimming performance of a biomimetic compliant fish-like robot. Exp Fluids 2009;47:927–939.
17. Marchese AD, Onal CD, Rus D. Autonomous soft robotic fish capable of escape maneuvers using fluidic elastomer actuators. Soft Robot 2014;1:75–87.
18. Lauder GV. Locomotion. In: The Physiology of Fishes, third edition. Evans DH, Claiborne JB. (Eds). Boca Raton, FL: CRC Press, 2006, pp. 3–46.
19. Mosadegh B, Poligerinos P, Keplinger C, Wennstedt S, *et al.* Pneumatic networks for soft robotics that actuate rapidly. Adv Funct Mater 2014;24:2163–2170.
20. Quinn DB, Lauder GV, Smits AJ. Flexible propulsors in ground effect. Bioinspir Biomim 2014;9:1–9.
21. Tytell ED, Lauder GV. The hydrodynamics of eel swimming. I. Wake structure. J Exp Biol 2004;207:1825–1841.
22. Wen L, Lauder GV. Understanding undulatory locomotion in fishes using an inertia-compensated flapping foil robotic device. Bioinspir Biomim 2013;8:046013.
23. Lauder GV, Anderson EJ, Tangorra J, Madden PGA. Fish biorobotics: kinematics and hydrodynamics of self-propulsion. J Exp Biol 2007;210:2767–2780.
24. McHenry MJ, Pell CA, Long JH. Mechanical Control of Swimming Speed: stiffness and axial form in undulating fish models. J Exp Biol 1995;198:2293–2305.
25. Long JH. Muscles, elastic energy, and the dynamics of body stiffness in swimming eels. Am Zool 1998;38:771–792.
26. Long JH, Adcock B, Root RG. Force transmission via axial tendons in undulating fish: a dynamic analysis. Comp Biochem Physiol Part A Mol Integr Physiol 2002;133:911–929.

27. Nowroozi BN, Brainerd EL. Importance of mechanics and kinematics in determining the stiffness contribution of the vertebral column during body-caudal-fin swimming in fishes. In Axial systems and their actuation: new twists on the ancient body of craniates. Zoology 2014;117:28–35.
28. Jayne BC, Lauder GV. New data on axial locomotion in fishes: how speed affects diversity of kinematics and motor patterns. Am Zool 1996;36:642–655.
29. Gillis GB. Undulatory locomotion in elongate aquatic vertebrates: anguilliform swimming since Sir James Gray. Am Zool 1996;36:656–665.
30. Tytell ED. The hydrodynamics of eel swimming II. Effect of swimming speed. J Exp Biol 2004;207:3265–3279.
31. Tytell ED, Leftwich MC, Hsu C, Griffith BE, Cohen AH, Smits AJ, *et al.* Role of body stiffness in undulatory swimming: insights from robotic and computational models. Phys Rev Fluids 2016;1:073202.

Address correspondence to:
Ardian Jusufi
Centre for Autonomous Systems
Faculty of Engineering and Information Technology
University of Technology, Sydney
CB 11.09.301
81 Broadway, Ultimo, NSW 2007
Australia

E-mail: ardian.jusufi@uts.edu.au